

The Central Regions of M81

T. J. Davidge & S. Courteau ^{1, 2}
 Herzberg Institute of Astrophysics,
 National Research Council of Canada,
 5071 W. Saanich Road, Victoria, BC Canada V8X 4M6
email: *tim.davidge@hia.nrc.ca, stephane.courteau@hia.nrc.ca*

ABSTRACT

High angular resolution near-infrared images, obtained with the Canada-France-Hawaii Telescope adaptive optics system, are combined with archival Hubble Space Telescope data to investigate the central regions of the nearby Sb galaxy M81 (NGC3031). The spectral-energy distribution of the circumnuclear region, which extends out to $1''.5$ (~ 24 pc if $\mu_0 = 27.5$) from the nucleus, can be modelled as a combination of an old metal-rich population and emission from hot dust. Thermal emission has been detected near other AGN, and simple models indicate that hot dust can account for $\sim 20\%$ of the light in K within $0''.5$ of the M81 nucleus. An elongated structure with $M_V \sim -7$, which may be an area of active star formation, is detected $0''.45$ from the nucleus. At distances in excess of $1''.5$ from the nucleus the $J - K$ color of the M81 bulge is not significantly different from what is seen in M31. The HST data are also used to search for bright globular clusters within 2kpc of the center of M81. The area within 0.26 kpc of the M81 nucleus is largely devoid of bright globular clusters, in agreement with what is seen in the central regions of the Galaxy and M31. However, our survey indicates that there may be $\sim 45 \pm 12$ globular cluster candidates with $M_V \leq -7$ within 2 kpc of the galaxy center, which is consistent with what would be inferred from the Milky-Way cluster system after adjusting for differences in the total number of clusters.

Key Words: galaxies: individual (NGC3031) – galaxies: nuclei – galaxies: Seyfert – galaxies: star clusters

¹Visiting Astronomers, Canada-France-Hawaii telescope, which is operated by the National Research Council of Canada, the Centre National de la Recherche Scientifique, and the University of Hawaii

²Guest Users, Canadian Astronomy Data Centre, which is operated by the Herzberg Institute of Astrophysics, National Research Council of Canada

1. INTRODUCTION

The central region of a galaxy lies at the bottom of a deep gravitational well, and physical processes such as dynamical friction, accretion, and dissipation of angular momentum can cause material to accumulate in this area that may provide insight into the past history of the host galaxy. In fact, there are indications that the evolutionary processes that defined the central characteristics of galaxies were major events that had a profound influence on the host systems (e.g. Faber *et al.* 1997). However, efforts to survey the stellar content near galaxy centers are frustrated by extremely high stellar densities, which not only make the detection of individual objects difficult, but can create environments that are systematically different from the solar neighborhood, thus complicating the interpretation of the results, even in the nearest systems. For example, the strength of $2.3\mu\text{m}$ CO absorption weakens within ~ 10 arcsec of SgrA* (Haller *et al.* 1996, Sellgren *et al.* 1990). There are a number of possible causes of this effect (Sellgren *et al.* 1990), including the stripping of stellar envelopes due to exposure to an intense radiation field, although current evidence favours the presence of an unresolved body of early-type stars (Eckart *et al.* 1995, Davidge *et al.* 1997a).

The Galactic Center (GC) may not be representative of the nuclear regions in other spiral galaxies. The nearest external spiral galaxy, M31, shows a complicated nuclear morphology (Lauer *et al.* 1993) that differs from the GC (Davidge *et al.* 1997b). While spectroscopic data are suggestive of an age gradient near the center of M31 (Davidge 1997), there is as yet no evidence for a population of very young stars, such as those in the SgrA complex, near the center of that galaxy. Clearly, it is important to survey the central regions of a larger sample of nearby galaxies at high angular resolutions to study nuclear morphology and search for evidence of recent star formation.

The central regions of M81 are of interest because this galaxy is one of the closest objects outside the Local Group, and has a morphological type similar to M31 (Sandage & Tammann 1987). In addition, the orientation of M81 leads to a clear view of the nucleus. Dynamical studies suggest that a central super-massive object is present (Keel 1989; Ho, Filippenko, & Sargent 1996), and M81 is the closest galaxy to show the spectroscopic signatures of Seyfert-1 and LINER activity (Ho *et al.* 1996; Keel 1989; Filippenko & Sargent 1988). There is nuclear radio emission originating from a compact area having projected dimensions $\leq 700 \times 300$ AU (Bienlenholz *et al.* 1996), and Falcke (1996) and Reuter & Lesch (1996) conclude that the M81 nucleus is a more energetic version of SgrA*. Spectroscopic studies predict that the narrow line region (NLR) is contained within a few arcsec (ie. a few tens of parsecs) of the nucleus (Filippenko & Sargent 1988), and the asymmetric profiles of forbidden lines indicate that sub-structures should be present in this

area (e.g. Keel 1989). However, previous investigations with the Hubble Space Telescope (HST) FOC and WFPC2 images at ultraviolet and visible wavelengths have shown only the central nucleus, with no evidence of sub-structure, star clusters, or a population of hot young stars (Devereux, Ford, & Jacoby 1997).

In the current paper, new high angular resolution near-infrared images are combined with existing HST data to explore the central regions of M81. Images recorded in the infrared are of interest since (1) they are relatively unaffected by all but the heaviest dust obscuration, (2) the contrast between the nuclear continuum emission, which has a blue spectral-energy distribution (SED), and the surrounding bulge is lower than at shorter wavelengths, simplifying the search for structures close to the nucleus, (3) there are prominent spectroscopic features, such as the $2.3\mu\text{m}$ CO bands, that are useful probes of stellar content and can be studied with narrow-band filters, and (4) emission from warm dust, which has been seen around other active galactic nuclei (e.g. Alonso-Herrero, Ward, & Kotilainen 1996), can be detected at these wavelengths.

2. OBSERVATIONS AND REDUCTIONS

Images were recorded through J , H , K , $\text{Br}\gamma$, CO, and $2.26\mu\text{m}$ continuum filters during the nights of UT March 7 – 8 1998 using the Canada-France-Hawaii Telescope (CFHT) Adaptive Optics Bonnette (AOB) (Rigaut *et al.* 1998) and KIR imager. KIR contains a 1024×1024 Hg:Cd:Te array with $0''.034 \text{ pix}^{-1}$. The CFHT AOB uses objects on the sky as reference beacons, and the M81 nucleus is sufficiently bright at visible wavelengths that it was employed for this purpose. A complete observing sequence consisted of either 2 or 4 exposures per filter at 4 dither positions that defined a $0''.5 \times 0''.5$ grid, and additional details of the observations are listed in Table 1. The FWHM entries in the last column of this table were measured from the point-like central nucleus of M81 after removing the underlying bulge light profile (§3). A field 1° North of the M81 center was observed periodically to monitor background sky brightness. Standard stars from Casali & Hawarden (1992) were also observed throughout the two night observing run. The photometric calibration of the J , H , and K M81 observations was verified by simulating the aperture measurements made by Willner *et al.* (1985), and we find excellent agreement with their published colors.

The data were reduced using the procedures described by Davidge *et al.* (1997a). The PSF in the final images consists of a bright central peak, with a width approaching that of the telescope diffraction limit for the images recorded near $2\mu\text{m}$, surrounded by an Airy pattern and faint satellite structures, which have been previously noted in AOB images by Chapman, Walker, & Morris (1998). We suspect that the latter are the consequence

of using an extended object as the AO reference source, as images of other fields, where stars were used as reference beacons, did not show these features. The absence of bright, isolated point sources in the M81 field prevented the use of deconvolution techniques to suppress the PSF satellites. Fortunately, although the presence of satellite structures in the PSF confounds efforts to search for faint sources close to the nucleus, the amplitude and location of the PSF satellites are not wavelength-sensitive, with the result that they are removed when images are ratioed. Consequently, the AOB data can be used to study the near-infrared SED of the M81 circumnuclear region at sub-arcsec angular scales.

Archival HST WFPC2 F547W and NIC2 F160W images of the center of M81 were extracted from the CADC HST database to search for faint sources close to the nucleus. The WFPC2 PC detector has a pixel scale of $0''.046 \text{ pix}^{-1}$, and samples a field comparable in size to that observed by KIR. The WF chips have $0''.1 \text{ pix}^{-1}$, and sample distances in excess of 2 arcmin from the nucleus. The WFPC2 data, which consist of frames U2JQ0301T, 2T, 3T, and 4T from program GO-5433, were pipeline processed using the CADC recalibration and median-combined. The NIC2 detector has a pixel scale of $0''.075 \text{ pix}^{-1}$, so that the angular sampling is roughly a factor of two coarser than that offered by KIR. The NICMOS observations, which consist of frames N3ZD0NYTQ, UQ, and VQ from program GO-7331, were pipeline processed and median combined.

3. RESULTS

3.1. The Circumnuclear Environment of M81

The $J - K$ color profile near the nucleus of M81 is shown in the top panel of Figure 1. The angular measurements plotted in this figure can be converted to spatial distances using the adopted distance modulus of $\mu_0 = 27.5$, so that $1''.0 = 15.3 \text{ pc}$. The K image was gaussian-smoothed to match the angular resolution of the J data, and the plotted points are azimuthal averages within $0''.2$ annuli. The error bars show the systematic uncertainties introduced by sky subtraction.

$J - K$ changes significantly within a few arcsec of the M81 nucleus, with the blue nuclear continuum producing a local minimum in the color profile at the galaxy center. The actual $J - K$ color of the central source is likely much smaller than that measured here, as seeing blurs our data and flattens color gradients. $J - K$ reaches a maximum when $r = 0''.4$, and at distances between $0''.5$ and $1''.5$ from the nucleus $J - K$ declines with radius, before levelling off at larger radii.

The $J - K$ color of M81 when $r \leq 1''.5$ is very different from that in the corresponding

region of M31. This is demonstrated in Figure 1, where M31 $J - K$ measurements from Mould *et al.* (1989), scaled along the horizontal axis to account for the greater distance to M81, are plotted as open squares. This comparison indicates that the circumnuclear region in M81 has a relatively red color when compared with M31. However, at distances in excess of $1''.5$ from the nucleus, the mean $J - K$ color of the M81 bulge agrees with that in M31, indicating a similarity in stellar contents.

The $(J - H, H - K)$ two-color diagram (TCD), plotted in the top panel of Figure 2, provides further evidence that the circumnuclear region of M81 has a SED that is very different from what is typically near the centers of bulges and early-type galaxies. The M81 data for points beyond $1''.5$ from the nucleus (open squares) overlap with the elliptical and S0 aperture measurements (crosses) made by Frogel *et al.* (1978), and fall slightly below the Baade's Window (hereafter BW) M giant sequence (solid line) as defined by Frogel & Whitford (1987). The M81 data for points within $1''.5$ of the nucleus, shown as filled squares, depart significantly from the BW M giant relation, and define a trend that is very different from the Galactic reddening vector, which is also shown in this figure. In §4 we demonstrate that the near-infrared SED of the circumnuclear region can be modelled as the sum of a stellar and non-stellar component, with the latter presumably due to hot ($T_{eff} \sim 1000$ K) dust.

The narrow-band CO, Br γ , and $2.26\mu\text{m}$ continuum images sample the longest wavelengths in the AOB dataset, and hence have higher Strehl ratios than the broad-band images. The modest difference in central wavelength between these three filters also means that any structure in the PSF is removed when any two images are ratioed. The radial distribution of the CO index, defined as $-2.5 \log(\text{CO}/2.26\mu\text{m} \text{ continuum})$ plus a zeropoint, is shown in the middle panel of Figure 1, where the plotted values are azimuthal averages in $0''.1$ annuli. The CO index weakens with decreasing radius when $r \leq 0''.5$. This is likely due to veiling of the CO features by non-photospheric emission (§4), as the near-infrared colors at these radii argue against a large population of early-type stars being present. The CO index has values appropriate for old, metal-rich populations when $r \geq 0''.6$, indicating that the light is predominantly photospheric at these radii.

The $(CO, J - K)$ TCD is shown in the lower panel of Figure 2. The CO indices plotted in this figure were measured after the CO and continuum images were gaussian smoothed to match the angular resolution of the J observations; therefore, the CO indices in Figure 2, especially those at small radii, differ from those in the middle panel of Figure 1, which were measured from unsmoothed images. When $r \geq 1''.5$ the M81 data occupy the same region of the TCD as early-type galaxies, and have smaller CO indices than bright giants in BW. At smaller radii the M81 data depart from the area occupied by early-type galaxies, and do

not follow the trend defined by the reddening vector. As with the $(J - H, H - K)$ TCD, this behaviour can be modelled as a combination of stellar and non-stellar components (§4).

Case B recombination theory predicts that the ratio of $\text{Br}\gamma$ and $\text{H}\alpha$ fluxes is roughly 0.01 (Giles 1977, Brocklehurst 1971), so that $\text{Br}\gamma$ emission can be weak and difficult to detect. While the moderately short integration times used here are probably not sufficient to detect circumnuclear $\text{Br}\gamma$ emission in M81, observations with the $\text{Br}\gamma$ filter still provide a means of probing the SED near $2\mu\text{m}$ at high angular resolutions, albeit over a relatively narrow wavelength range.

The radial behaviour of the instrumental $\text{Br}\gamma$ index, defined as $-2.5 \log(\text{Br}\gamma/2.26\mu\text{m}$ continuum), is shown in the lower panel of Figure 1, where azimuthal averages in $0''.1$ annuli are plotted. The $\text{Br}\gamma$ and $J - K$ color profiles have qualitatively similar behaviour when $r \geq 0''.3$, suggesting that the $\text{Br}\gamma$ index and $J - K$ track similar light sources at these radii, although the $\text{Br}\gamma$ curve shows sharper structure, due to the higher angular resolution of these data. The difference in angular resolution is most apparent near the nucleus, where the $\text{Br}\gamma$ index dips below the value seen at $2''.0$, whereas $J - K$ near the nucleus is redder than what is seen at larger radii.

Studies of any resolved objects in the circumnuclear region of M81 may provide additional clues into the nature of this area. Devereux *et al.* (1997) used F547M images centered on a WFC2 wide-field array ($0''.1 \text{ pix}^{-1}$) to search for faint sources near the center of M81 with negative results. The F547M/PC data considered here have finer pixel sampling, and hence are better suited to probing the circumnuclear regions of this galaxy. However, the bright nucleus and steep bulge brightness profile near the center of M81 complicate efforts to search for faint objects. Light from the bulge was removed by first smoothing the PC image with a running median filter, and then subtracting the smoothed frames from the initial image. The smoothing length was set at twice the FWHM, and experiments with different smoothing lengths indicated that the ability to detect faint sources was not affected by this parameter. The nucleus was subtracted by assuming that it is a radially symmetric point source.

The central $3''.4 \times 3''.4$ (52×52 pc) portion of the F547M/PC image, with the bulge and nucleus removed using the procedure described above, is shown in Figure 3. A number of point sources, the brightest of which are marked with squares and circles, are present in this figure. These sources may not be single luminous stars, but could be resolution elements that contain a fortuitous concentration of moderately bright giants. One way to estimate the amplitude of such stellar content fluctuations is to measure the random noise level which, because of the high central surface brightness of M81, is dominated by these events. Adopting a conservative criterion that only those sources exceeding the random

noise level by 5σ are physically real objects, so that only a single noise event may be mis-identified as a star in the KIR field, then almost all the sources marked in Figure 3 are likely stellar content fluctuations and not single bright objects; indeed, the sources marked with squares in Figure 3, which have $V \sim 23 \pm 0.5$ based on the calibration of Holtzman *et al.* (1995), exceed the background noise at only the 4σ level. There is one exception, which is the extended object, or group of objects, marked with the circle and located $0''.45$ northeast of the main nucleus. This source has $V \sim 20.5 \pm 0.5$, and exceeds the noise level by 30σ . Consequently, there is a very good chance that it is a physically real object and not a fluke superposition of stars.

Another way to evaluate the amplitude of stellar content fluctuations near the M81 nucleus is to co-add fields at larger radii to simulate areas of higher surface brightness. Experiments of this nature further confirm that the objects marked with the squares in Figure 3 are likely stellar content fluctuations, and not individual bright sources. These experiments were unable to reproduce an object like that $0''.45$ northeast of the nucleus, providing further evidence that it is a real source.

The F160W/NIC2 image, with the bulge and central source removed using the procedure described above, is shown in Figure 4. The extended source $0''.45$ northeast of the nucleus is clearly evident in Figure 4, adding further confidence that this is a real object.

3.2. A Search for Globular Clusters in the Inner Bulge of M81

Crowding makes it difficult to resolve even the most luminous red giants near the centers of galaxies outside the Local Group. However, globular clusters are sufficiently bright that they should be visible in relatively high-density environments. The globular clusters that have been discovered in the central regions of the Milky Way are compact, with half light radii in the range $1 - 2$ pc (van den Bergh 1994). Objects such as these would subtend $0''.06 - 0''.12$ at the distance of M81, and hence would appear as slightly extended sources in the F547M WFPC2 data. With a typical brightness of $M_V \sim -7$, bright globular clusters would thus appear as 10σ sources with respect to stochastic fluctuations in stellar content near the center of M81; consequently, it is likely that the fluctuations with $V \sim 23$ marked in Figure 3 are not globular clusters.

Devereux *et al.* (1997) concluded that there are no globular clusters within $2''$ of the M81 nucleus, and the archival WFPC2 data can be used to extend this search to a much larger area. The HST F547W/PC image, which covers a $37'' \times 37''$ area, was searched for globular clusters after removing the bulge light profile using the procedure described in §3.1.

The FIND routine in DAOPHOT (Stetson 1987), with the ‘sharp’ and ‘round’ parameters set to permit elongated and extended objects to be detected, was used to construct a preliminary list of objects. Only sources that had at least one pixel exceeding the background noise level at the 5σ level were retained to avoid detecting stochastic fluctuations in stellar content. The radial light profile of each object was then examined by eye to classify the sources as either stellar or extended. The brightnesses of individual objects were measured with the DAOPHOT aperture photometry routine PHOT. Only one extended object, located $15''.6$ north west of the nucleus, was found outside the circumnuclear region in the PC field. This source has $V=20.2$, which corresponds to $M_V = -8.2$ if $A_V = 0.9$ mag (Perelmutter & Racine 1995). Younger star clusters and HII regions will also appear as extended objects and, lacking the color information needed to identify such sources, we can not unambiguously state whether or not this object is a bright globular cluster.

A larger population of globular cluster candidates have been discovered with the three WF detectors. Neglecting obvious bright foreground stars, the technique described above finds 25 sources with $V \leq 21.5$, which is the estimated completeness limit of these data, and 15 of these are extended objects. The WFPC2 field covers $\sim 1/3$ of the projected area within $139''.0$ (~ 2 kpc) from the center of M81. Consequently, we estimate that there are $3 \times 15 \pm 4 = 45 \pm 12$ extended objects with $M_V \leq -7$ within 2 kpc of the galaxy center.

4. DISCUSSION AND SUMMARY

Near-infrared images obtained with the CFHT adaptive optics system have been combined with archival HST data to investigate the central regions of the nearby spiral galaxy M81. Studies of the central forbidden emission line spectrum of this galaxy predict that kinematically distinct structures (Filippenko & Sargent 1988, Keel 1989) and significant density stratification (Ho *et al.* 1996) should occur in the NLR, which may extend out to a few arcsec from the nucleus (Filippenko & Sargent 1988). We find that the near-infrared SED near the M81 nucleus changes with radius, providing additional evidence of stratification in the circumnuclear interstellar medium. $J - K$ peaks $\sim 0''.4$ from the nucleus, at a value that is significantly redder than what is seen in the corresponding portion of M31, although at $1''.5$ from the nucleus M31 and M81 have similar $J - K$ colors. The CO index near the nucleus is relatively weak, indicating that the red $J - K$ color is not due to a population of extremely red stars.

The near-infrared SED of the M81 circumnuclear region can be reproduced with a simple two component model, in which emission from warm dust, which is a common occurrence in LINER (Wilner *et al.* 1985) and Seyfert (Alonso-Herrero *et al.* 1996, and

references therein) systems, is added to a stellar component. Following Alonso-Herrero *et al.* (1996), we have generated model SEDs for various mixtures of dust and stars, and the results are shown as dashed lines in Figure 2. The near-infrared colors of the stellar component were fixed at the values in M81 1''.5 from the nucleus, while the dust is assumed to follow a black-body curve with a temperature of 1000K. The dust temperature is based on observations of other Seyferts at longer wavelengths (Alonso-Herrero *et al.* 1996), although at near-infrared wavelengths the model SEDs are insensitive to this parameter.

The simple two component models reproduce the trends defined by the observations on the $(J - H, H - K)$ and $(CO, J - K)$ TCDs, and predict that 20% of the light in K within 0''.5 of the M81 nucleus originates from warm dust. At small distances from the nucleus the observations deviate from the predicted trend, due to continuum emission from the nuclear source. The presence of hot dust near the center of M81 is yet another example of how this galaxy harbours a small-scale version of the engines that occur in more powerful systems.

The central regions of AGNs are morphologically complex environments (e.g. Malkan, Gorjian, & Tam 1998), and we have used archival F547M and F160W HST images to find a faint extended object in the M81 NLR with $V \sim 20.5$, which corresponds to $M_V \sim -7.3$ if $A_V = 0.3$ (Filippenko & Sargent 1988) and $\mu_0 = 27.5$. The complicated PSF in the CFHT images makes it difficult to investigate this structure with these data, and the nature of this object remains a matter of speculation. However, the fact that it is detected in both the WFPC2 and NIC2 datasets suggests that it has a flat SED, so a source dominated solely by either very red or blue stars can be ruled out. There is evidence for recent star formation in the central regions of Seyfert-1 galaxies (e.g. Gonzalez Delgado & Perez 1997), and we speculate that this object could be an HII region. High angular resolution spectra at optical wavelengths, which would allow key diagnostics such as $H\alpha$ and [OIII] emission to be studied, will provide insight into the nature of this object. The detection of a star-forming region near the center of M81 may have implications for the origins of the young stellar complexes that are found within a few tens of pc of the GC (e.g. Morris & Serabyn 1996, and references therein).

We have also searched for globular clusters in the central regions of M81. This galaxy is an interesting target for studying the central globular cluster content of spiral galaxies as it is relatively close while the inner regions are more-or-less free of the absorption that plagues efforts to survey the corresponding area of the Milky Way. Perelmutter & Racine (1995) investigated the global properties of the M81 globular cluster system, and found that the spatial distribution of clusters at large radii is similar to that of the Galactic and M31 globular cluster systems. However, the Perelmutter and Racine (1995) survey excluded the

region within 1 arcmin of the nucleus, so it is not known if there is an absence of globular clusters near the galaxy center, as is the case in the Milky-Way and M31 (Battistini *et al.* 1993).

Using archival WFPC2 data, we estimate that there are $\sim 45 \pm 12$ extended objects with $M_V \leq -7$, many of which will be globular clusters, within 2 kpc of the galaxy center. For comparison, there are 17 clusters with $M_V \leq -7$ within 2kpc of the Galactic Center (Harris 1996). The M81 cluster system is 1.4 ± 0.2 times more populous than that in the Milky-Way (Perelmutter & Racine 1995), so 24 ± 3.4 globular clusters would be expected within 2 kpc of the center of M81 if the central spatial distributions of the M81 and Galactic cluster systems scaled according to total cluster population. Given that the difference between the observed and predicted number of clusters, 21 ± 13 , is significant at less than the 2σ level, and that some of the extended objects detected in M81 will not be globular clusters, these data support the hypothesis that the central spatial distributions of the two cluster systems are similar.

There is only one globular cluster candidate within 0.27 kpc of the center of M81, suggesting that the number density of clusters does not build towards very small radii in this galaxy. The near absence of bright globular clusters within a few 100 pc of the centers of M31 and M81, the nearest large external spiral galaxies, strongly suggests that the dearth of clusters in the corresponding part of the Galaxy is a real effect, and not an artifact of extinction-induced incompleteness or a statistical fluke.

It is not clear if a single physical mechanism is responsible for the absence of globular clusters near the centers of spiral galaxies. Murali & Weinberg (1997) and Vesperini (1997) argue that dynamical processes play a major role in shaping the observed properties of the Galactic cluster system, and that clusters which formed in the innermost regions of the Galaxy have been disrupted. However, the central globular cluster content in elliptical galaxies is deficient with respect to the underlying galactic light, and the Milky-Way cluster system falls along the relation between system core radius and galaxy luminosity defined by early-type galaxies (Forbes *et al.* 1996), suggesting that the processes that shaped the properties of the globular cluster systems in the Milky-Way and elliptical galaxies are related. This connection is significant because Lauer & Kormendy (1986) argue that the spatial distribution of globular clusters in very large ellipticals, such as M87, can not be the result of dynamical friction, and hence may have been imprinted at early epochs. Nevertheless, Lauer & Kormendy (1986) also note that dynamical friction will still be a factor for clusters located well within the globular cluster system core radius. The absence of clusters near the centers of nearby spiral galaxies may thus be the result of the combined effects of an initially low central cluster density that was subsequently culled by dynamical

effects.

Sincere thanks are extended to Sidney van den Berg, Jim Hesser, Simon Morris, and Sylvain Veilleux for commenting on an earlier draft of this paper. An anonymous referee also made suggestions that greatly improved the manuscript. Thanks are also extended to Daniel Durand and Severin Gaudet for providing the pipeline-processed NICMOS data used in this paper.

Filter	Exposure Time (sec)	FWHM (arcsec)
J	16 × 90	0.34
H	16 × 90	0.31
K	16 × 90	0.20
Br γ	8 × 60	0.17
2.26 μ m continuum	8 × 60	0.17
CO	8 × 90	0.17

Table 1: DETAILS OF OBSERVATIONS

REFERENCES

Alonso-Herrero, A., Ward, M. J. & Kotilainen, J. K. 1996, MNRAS, 278, 902

Bartel, N. *et al.* 1982, ApJ, 262, 556

Battistini, P. L. *et al.* 1993, A&Ap, 272, 77

Bessell, M. S., & Brett, J. M. 1988, PASP, 100, 1134

Bietenholz, M. F. *et al.* 1996, ApJ, 604

Brocklehurst, M. 1971, MNRAS, 153, 471

Casali, M., & Hawarden, T. 1992, UKIRT-JCMT Newsletter, 4, 33

Chapman, S. C., Walker, G. A. H., & Morris, S. L. 1998, astro-ph 9810250

Davidge, T. J. 1997, AJ, 113, 985

Davidge, T. J. 1998, AJ, 115, 2374

Davidge, T. J., Simons, D. A., Rigaut, F., Doyon, R., & Crampton, D. 1997a, AJ, 114, 2586

Davidge, T. J., Rigaut, F., Doyon, R., & Crampton, D. 1997b, AJ, 113, 2586

Devereux, N., Ford, H., & Jacoby, G. 1997, ApJ, 481, L71

Eckart, A., Genzel, R., Hofmann, R., Sams, B. J., & Tacconi-Garman, L. E. 1995, ApJ, 445, L23

Elias, J. H., Frogel, J. A., & Humphreys, R. M. 1985, APJS, 57, 91

Faber *et al.* 1997, AJ, 114, 1771

Falcke, H. 1996, ApJ, 464, L67

Filippenko, A. V., & Sargent, W. L. W. 1988, ApJ, 324, 134

Forbes, D. A., Franx, M., Illingworth, G. D., & Carollo, C. M. 1996, ApJ, 467, 126

Frogel, J. A., & Whitford, A. E. 1987, ApJ, 320, 199

Frogel, J. A., Persson, S. E., Aaronson, M., & Matthews, K. 1978, ApJ, 220, 75

Giles, K. 1977, MNRAS, 180, 57P

Gonzalez Delgado, R. M., & Perez, E. 1997, MNRAS, 284, 931

Haller, J. W., Rieke, M. J., Rieke, G. H., Tamblyn, P., Close, L. & Melia, F. 1996, ApJ, 456, 194

Harris, W. E. 1996, AJ, 112, 1487

Ho, L. C., Filippenko, A. V., & Sargent, W. L. W. 1996, ApJ, 462, 183

Holtzman, J. A., *et al.* 1995, PASP, 107, 1065

Keel, W. C. 1989, AJ, 98, 195

Krabbe, A. et al. 1995, ApJ, 447, L95

Larkin, J. E., Armus, L., Knop, R. A., Soifer, B. T., & Matthews, K. 1998, ApJS, 114, 59

Lauer *et al.* 1993, AJ, 106, 1436

Lauer, T. R., & Kormendy, J. 1986, ApJ, 303, L1

Malkan, M. A., Gorjian, V., & Tam, R. 1998, ApJS, 117, 25

Morris, M., & Serabyn, E. 1996, ARAA, 34, 645

Mould, J., Graham, J., Matthews, K., Soifer, B. T., & Phinney, E. S. 1989, ApJ, 339, L21

Murali, C., & Weinberg, M. D. 1997, MNRAS, 288, 749

Perelmutter, J-M, & Racine, R. 1995, AJ, 109, 1055

Reuter, H.-P., & Lesch, H. 1996, A&A, 310, L5

Rieke, G. H., & Lebofsky, M. J. 1985, ApJ, 288, 618

Rigaut, F. *et al.* 1998, PASP, 110, 152

Sandage, A., & Tammann, G. A. 1987, A Revised Shapley-Ames Catalog of Galaxies, Carnegie, Washington DC.

Sellgren, K., McGinn, M. T., Becklin, E. E., & Hall, D. N. B. 1990, ApJ, 359, 112

van den Bergh, S. 1994, AJ, 108, 2145

Vesperini, E. 1997, MNRAS, 287, 915

Willner, S. P., Elvis, M., Fabbiano, G., Lawrence, A., & Ward, M. J. ApJ, 299, 443

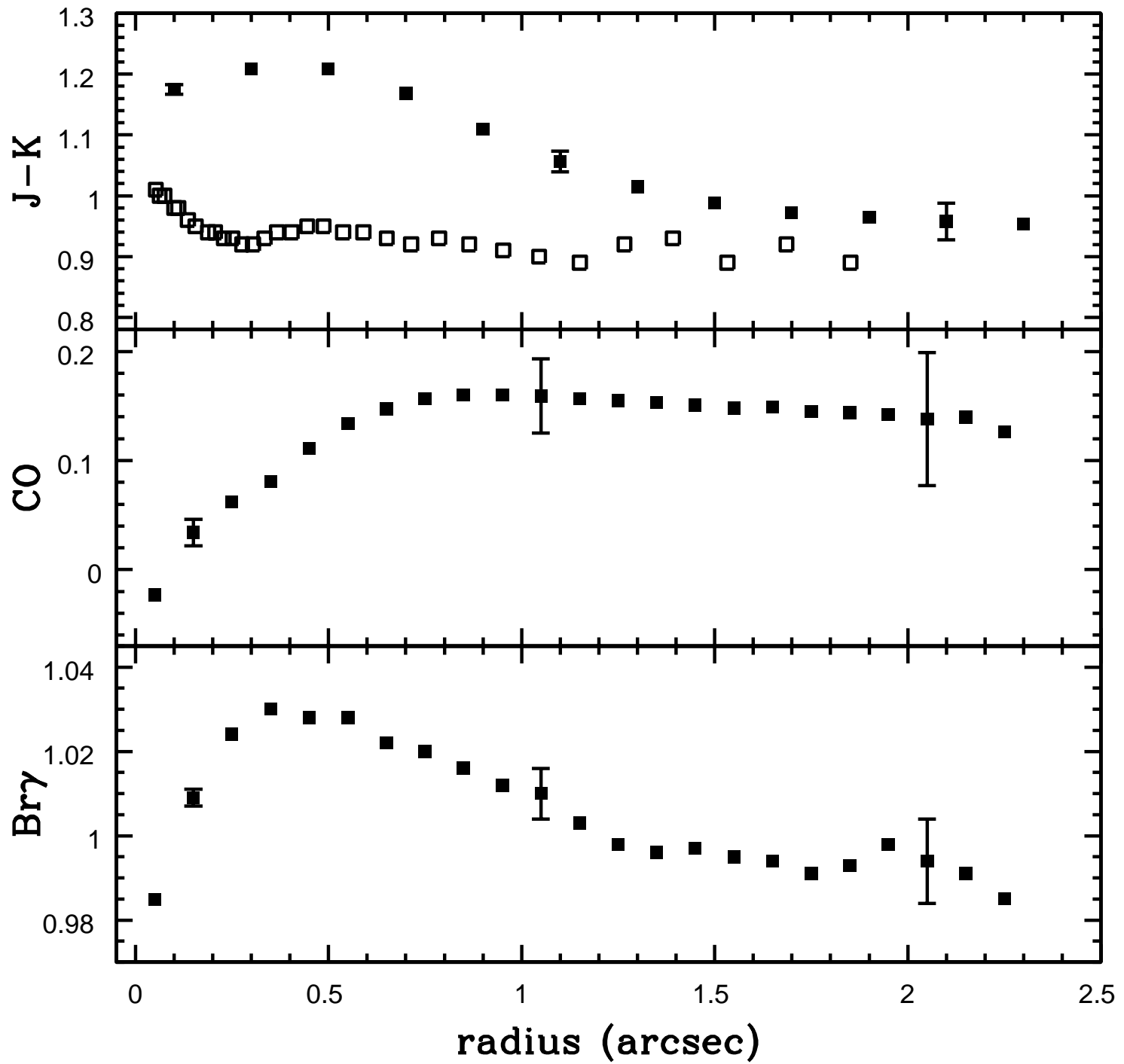
FIGURE CAPTIONS

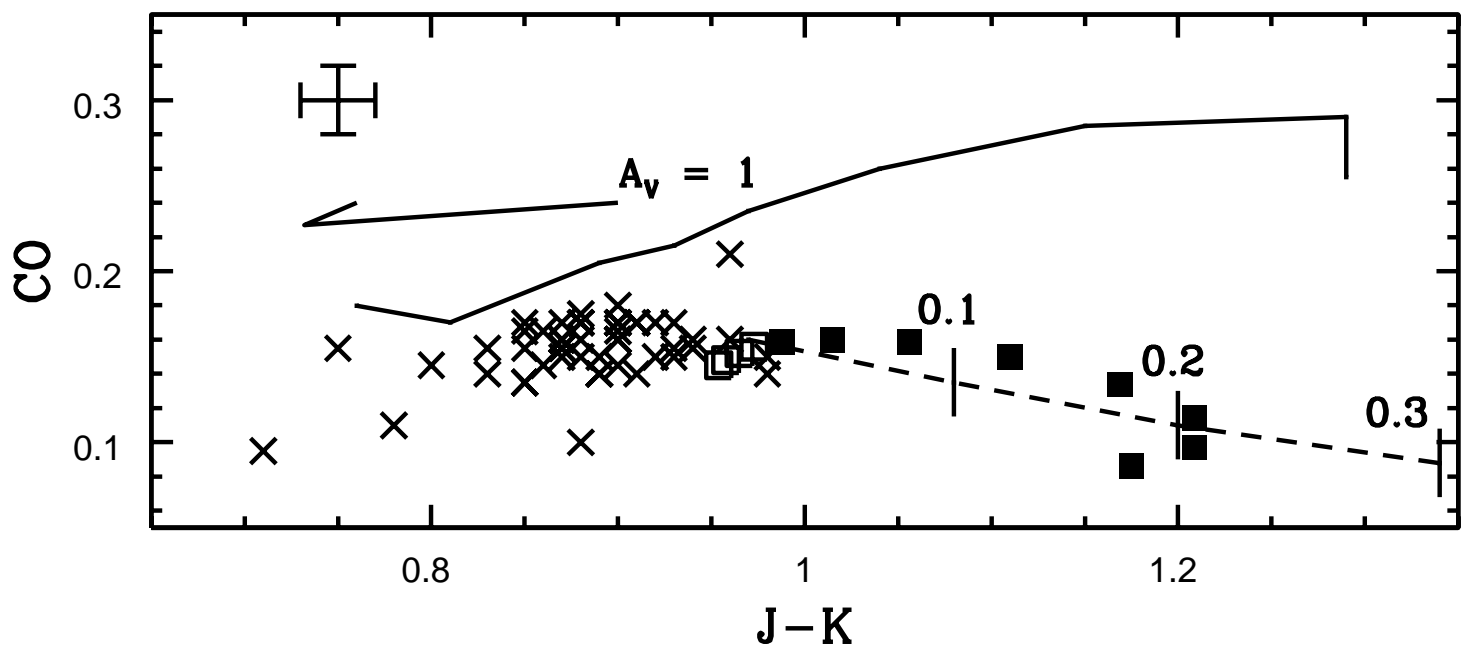
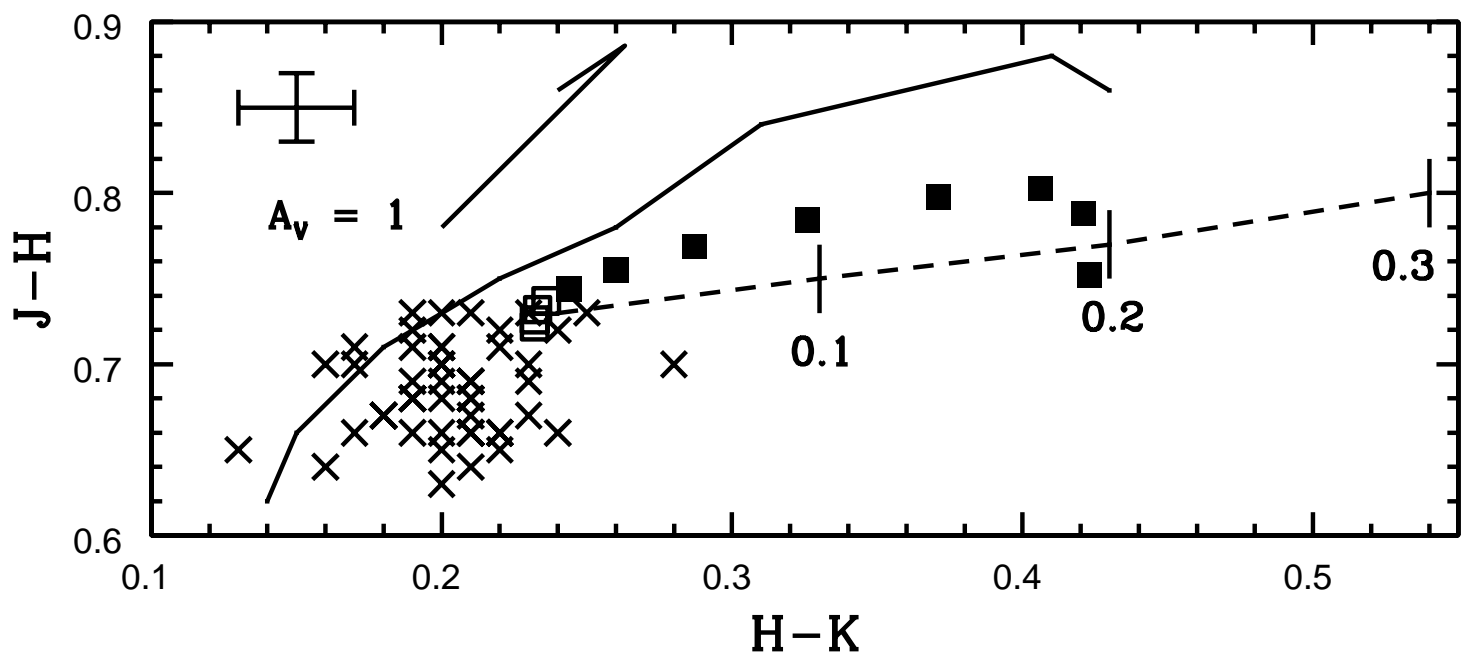
Fig. 1.— Radial $J - K$, CO, and $\text{Br}\gamma$ profiles near the center of M81, with distance measured from the galaxy nucleus. The M81 data, shown as solid squares, are azimuthal averages, and the error bars show the systematic errors introduced by uncertainties in the background. The open squares in the top panel are major axis color measurements for M31 taken from Table 1 of Mould *et al.* (1989), shifted to the distance of M81 by assuming that $\mu_0^{M31} = 24.5$ and $\mu_0^{M81} = 27.5$. The CO and $\text{Br}\gamma$ indices are in magnitude units, with the latter in the instrumental system.

Fig. 2.— $(J - H, H - K)$ and $(\text{CO}, J - K)$ diagrams for the central regions of M81. The data plotted are azimuthal averages in $0''.2$ annuli centered on the M81 nucleus with filled and open squares referring to distances $\leq 1''.5$ and $\geq 1''.5$ from the galaxy center, respectively. There is almost a one-to-one correspondence between color and distance from the M81 nucleus, in the sense that points with the largest $H - K$ and $J - K$ values are closest to the galaxy center. Also shown are measurements for elliptical and S0 galaxies from Table 4 of Frogel *et al.* (1978) (crosses), and the trend defined by M giants in BW from Table 3B of Frogel & Whitford (1987) (solid line). The error bar in each panel shows the 1σ uncertainties in the photometric zeropoints derived from the standard star measurements. Reddening vectors with lengths appropriate for $A_V = 1$ mag, based on the Rieke & Lebofsky (1985) reddening curve and $E(\text{CO})/E(B - V) = -0.04$ (Elias, Frogel, & Humphreys 1985), are shown. The dashed lines show the effects of combining the near-infrared SED of M81, as inferred from data at radii in excess of $1''.5$ from the nucleus, with a $T_{eff} = 1000$ K black-body. Points showing ratios of black-body to stellar flux of 0.1, 0.2, and 0.3 in K are marked.

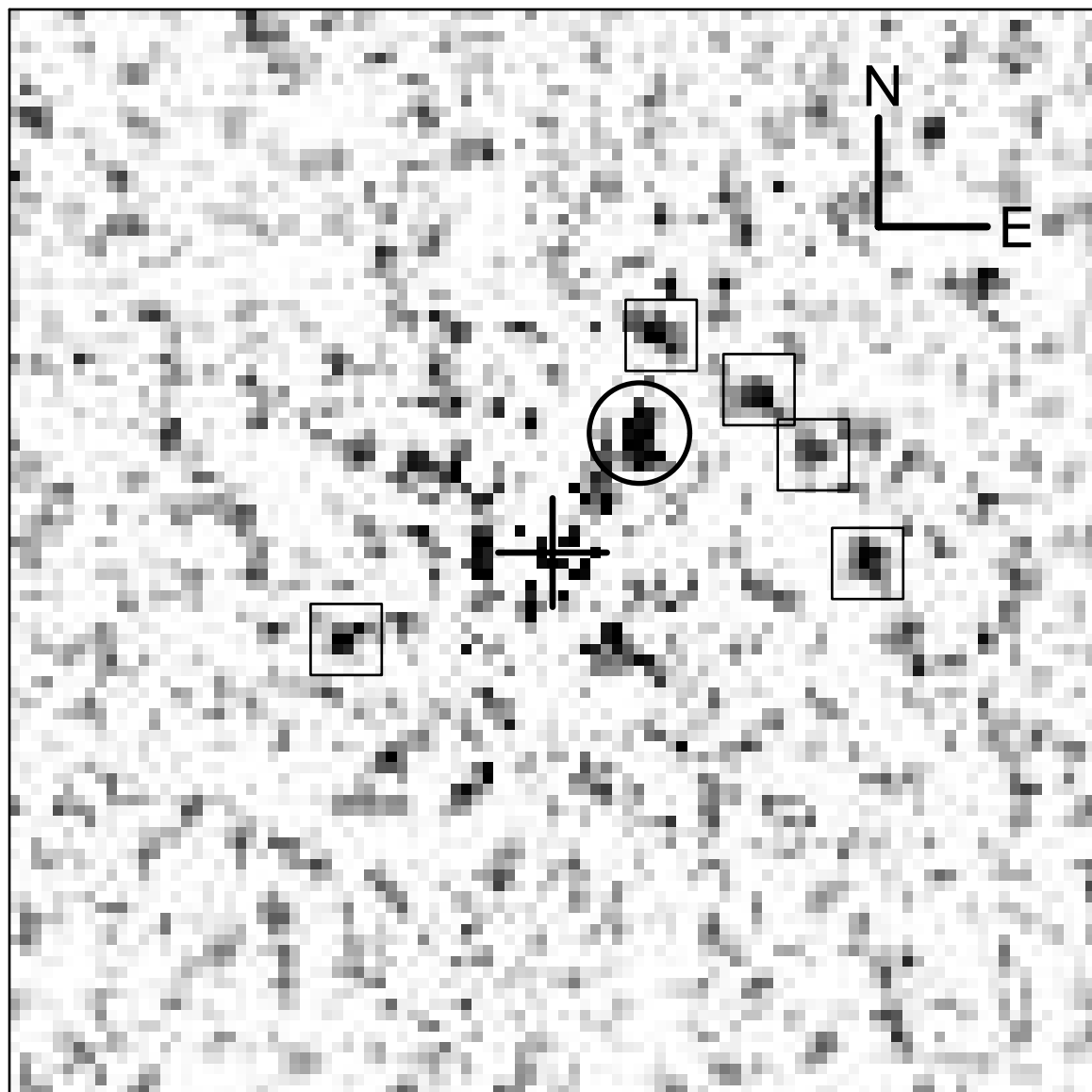
Fig. 3.— The portion of the F547M Planetary Camera image showing the central $3''.4 \times 3''.4$ (52×52 pc) of M81. The bulge light profile and the central nuclear source have been removed using the procedure described in the text, and the cross marks the center of M81. North is at the top, and east is to the right. The brightest objects have the darkest colors. The extended object marked with a circle is located $0''.45$ north east of the nucleus, and exceeds the random noise in the background at the 30σ level. The squares indicate the next five brightest objects in the field, which are likely stochastic fluctuations in stellar content, rather than individual bright stars.

Fig. 4.— The portion of the F160W NIC2 image that corresponds to the field shown in Figure 3. The bulge light profile and the central nuclear source have been removed using the procedure described in the text, and the cross marks the center of M81. North is at the top, and east is to the right. The brightest objects have the darkest colors. The circle marks the extended object indicated in Figure 3, which is located $0''.45$ north east of the nucleus.





M81 WFPC2 data



M81 NIC2 data

